

A Unified Wall Boundary Treatment for Viscous and Inviscid Flows in the CE/SE Method

S-C Chang¹, Z-C Zhang², S.T. John Yu² and P.C.E. Jorgenson¹

¹ NASA Glenn Research Center, Cleveland, OH

² Mechanical Engineering Department, Wayne State University, Detroit, MI

Abstract. In the setting of the CE/SE method, a new and unified wall boundary treatment for the Navier-Stokes and Euler Equations is proposed. In essence, the shear stress exerted on the fluid by a wall is modeled as a source term as a part of local space-time flux conservation in the vicinity of a wall boundary. When the fluid is inviscid, the source term vanishes and the boundary condition reduces to the usual "slip" condition. On the other hand, when the fluid is viscous, the source-term effect is consistent with the traditional no-slip condition. Numerical results show that the new treatment is robust, efficient and accurate for viscous and inviscid flows.

1. Introduction

In conventional CFD, the slip condition is applied along the wall for inviscid flows, while no-slip condition is applied for viscous flows. In this paper, a unified wall boundary treatment for inviscid and viscous flows is proposed in the setting of the CE/SE method [1-3]. In essence, the shear stress exerted on the fluid by a wall is modeled as a source term as a part of local space-time flux conservation in the vicinity of a wall boundary. When the fluid is inviscid, the source term vanishes and the boundary condition reduces to the usual "slip" condition. On the other hand, when the fluid is viscous, the source-term effect is consistent with the traditional no-slip condition. The accuracy, efficiency and robustness of the new boundary treatment is demonstrated using numerical examples in which reflection of an oblique shock on a wall is calculated for both viscous and inviscid flows.

2. The CE/SE Scheme for 2D Viscous Flows

The 2D Navier-Stokes Equations in conservation form can be written as

$$\frac{\partial u_m}{\partial t} + \frac{\partial f_{im}}{\partial x} + \frac{\partial g_{im}}{\partial y} - \frac{\partial f_{vm}}{\partial x} - \frac{\partial g_{vm}}{\partial y} = 0, \quad m=1,2,3,4 \quad (1)$$

The column matrices formed by $u_m, f_{im}, g_{im}, f_{vm}, g_{vm}$, $m=1,2,3,4$, respectively, are:

$$\begin{aligned}
U &= \begin{bmatrix} \rho \\ \rho u \\ \rho v \\ E_t \end{bmatrix} \quad F_i = \begin{bmatrix} \rho u \\ \rho u^2 + p \\ \rho uv \\ \rho uv \\ (E_t + p)u \end{bmatrix} \quad G_i = \begin{bmatrix} \rho v \\ \rho uv \\ \rho v^2 + p \\ (E_t + p)v \end{bmatrix} \\
F_v &= \begin{bmatrix} 0 \\ \tau_{xx} \\ \tau_{xy} \\ \tau_{xy}u + \tau_{yy}v - q_x \end{bmatrix} \quad G_v = \begin{bmatrix} 0 \\ \tau_{xy} \\ \tau_{yy} \\ \tau_{xy}u + \tau_{yy}v - q_y \end{bmatrix}
\end{aligned} \tag{2}$$

The inviscid fluxes f_{im} , g_{im} are functions of u_m , while the viscous fluxes f_{vm} and g_{vm} are functions of u_m , $\partial u_m / \partial x$ and $\partial u_m / \partial y$. Let $x_1 = x$, $x_2 = y$ and $x_3 = t$ be the coordinates of a Euclidean space E_3 . Then the conservation form of Eq. (1) is

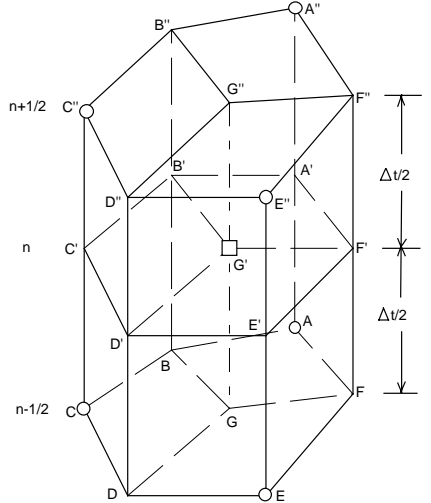
$$\oint_{S(V)} \vec{h}_m \cdot d\vec{s} = 0 , \quad m = 1, 2, 3, 4 \tag{3}$$

where (i) $\vec{h}_m = (f_{im}, f_{vm}, g_{im}, g_{vm}, u_m)$, (ii) $S(V)$ is the boundary of a region V in E_3 , (iii) $d\vec{s} = d\sigma \vec{n}$ with $d\sigma$ and \vec{n} , respectively, being the area and outward unit normal of a surface element on $S(V)$. \vec{h}_m can be decomposed into the inviscid and viscous parts, i.e.,

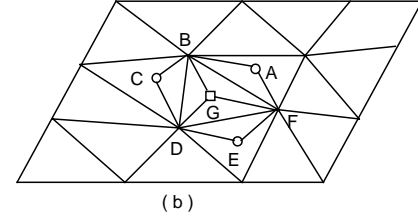
$$\vec{h}_m = \vec{h}_{im} - \vec{h}_{vm} \tag{4}$$

where $\vec{h}_{im} = (f_{im}, g_{im}, u_m)$, and $\vec{h}_{vm} = (f_{vm}, g_{vm}, 0)$.

In the 2D CE/SE method [2], the space-time mesh used (Fig.1(a)) is constructed from a spatial triangle mesh (Fig.1(b)). The unknowns are stored at the space-time mesh points (marked by squares and circles in Fig.1(a)) with their spatial projections being the centroids of the triangles depicted in Fig.1(b). Each space-time mesh point is associated with three conservation elements (CEs) and one solution element (SE). As an example, at point G' , the associated CEs are cylinders $E'F'G'D'EFGD$ ($CE^{(1)}$), $A'B'G'F'ABGF$ ($CE^{(2)}$) and $C'D'G'B'CDGB$ ($CE^{(3)}$). The SE is the union of four planes $A'B'C'D'E'F'$, $GG''B''B$, $GG''D''D$ and $GG''F''F$, and their immediate neighborhood. As explained in [2], inside each SE (such as that associated with point G'), u_m, f_{im}, g_{im}



(a)



(b)

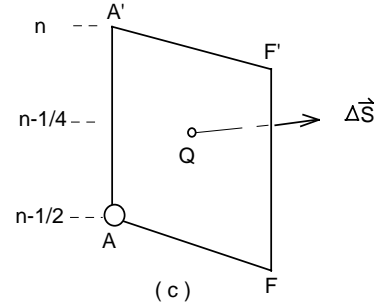


Fig. 1 A schematic of the CE/SE scheme: (a) a space-time mesh; (b) a triangular spatial mesh; (c) calculation of viscous fluxes.

are approximated by first-order Taylor's expansions in x , y and t with the expansion coefficients being functions of the independent unknowns $(u_m)_{G'}$, $(u_{mx})_{G'}$ and $(u_{my})_{G'}$. By imposing numerical analogues of Eq. (3) over CEs and using other conditions, a family of CE/SE Euler solvers, referred to as the Euler $\alpha\text{-}\epsilon\text{-}\alpha\text{-}\beta$ schemes, is constructed in [2]. Since the current Navier-Stokes solver is an extension of the Euler $\alpha\text{-}\epsilon\text{-}\alpha\text{-}\beta$ scheme with additional treatments of the viscous terms, only these additional treatments will be discussed in this paper.

To proceed, note that the third (time) component of each \vec{h}_{vm} vanishes. Thus, in calculating the total viscous flux leaving a CE (such as CE⁽²⁾) through its boundary, we only need to evaluate the viscous fluxes leaving the CE through its four lateral surfaces ABA'B', BGB'G', GFG'F' and FAF'A'. To explain how they are evaluated, as an example, we consider the surface FAF'A' (Fig.1(c)). Let $\Delta\vec{S} = (S_x, S_y, 0)$ be the unit outward normal vector of FAF'A' multiplied by its area. Then

$$\int_{FAF'A'} \vec{h}_{vm} \cdot d\vec{s} \approx S_x \cdot f_{vm}((u_m)_Q, (u_{mx})_Q, (u_{my})_Q) + S_y \cdot g_{vm}((u_m)_Q, (u_{mx})_Q, (u_{my})_Q) \quad (5)$$

where Q denotes the centroid of FAF'A'. Because FAF'A' belongs to the SE of point A, we assume that

$$(u_m)_Q \approx (u_m)_A + (u_{mx})_A(x_Q - x_A) + (u_{my})_A(y_Q - y_A) + (u_{mt})_A \cdot \Delta t / 4 \quad (6)$$

Note that, as explained in [2], $(u_{mt})_A$ is a function of the independent unknowns $(u_m)_A$, $(u_{mx})_A$ and $(u_{my})_A$. Furthermore, it is assumed that

$$(u_{mx})_Q \approx (u_{mx})_A, \quad (u_{my})_Q \approx (u_{my})_A \quad (7)$$

Since the above scheme is constructed using a triangular mesh, it is compatible with unstructured meshes. In addition, the above scheme has been extended to become a three-dimensional NS solver, which however is beyond the scope of this paper.

3 Unified Wall Boundary Treatment

For simplicity, consider the horizontal wall depicted in Fig. 2(a). No grid point is placed on the wall. Instead, a ghost point E, which is the mirror image of point G with respect to the wall, is introduced. The flow variables u_m and their spatial derivatives, u_{mx} and u_{my} ($m=1, 2, 3, 4$), at point E

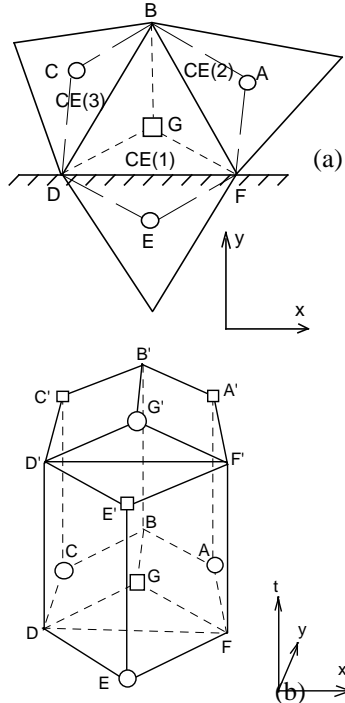


Fig.2. A schematic for wall boundary treatment: (a) a spatial mesh and (b) CEs near the wall boundary.

are obtained from those of point G by assuming that, at any time t , the flow fields below and above \overline{DF} are the mirror images of each other, i.e., we have

$$\begin{cases} (u_m)_E = (u_m)_G & m = 1,2,4 \\ (u_m)_E = -(u_m)_G & m = 3 \end{cases} \quad \begin{cases} (u_{mx})_E = (u_{mx})_G & m = 1,2,4 \\ (u_{mx})_E = -(u_{mx})_G & m = 3 \end{cases} \quad \begin{cases} (u_{my})_E = -(u_{my})_G & m = 1,2,4 \\ (u_{my})_E = (u_{my})_G & m = 3 \end{cases} \quad (8)$$

Using the above conditions and the concepts of the dual space-time mesh discussed in [2], one can calculate the flow variables and their spatial derivatives at G for the next time step. The calculation involves an integration over three conservation elements $CE^{(i)}$, $i = 1,2,3$ (Fig. 2(b)). However, a special treatment for the calculation in $CE^{(1)}$ is needed due to the wall boundary lying across $CE^{(1)}$.

Let (i) the viscosity μ be a constant; (ii) the wall be an insulated wall; (iii) S be the area of the rectangle DFF'D'; (iv) Q_+ and Q_- , respectively, be the points immediately above and below the centroid Q of DFF'D'. Then, because (i) $u = v = 0$ at the wall; and (ii) the numerical solution is linear in x , y , and t within a SE, the mass, momentum and energy fluxes entering into the fluid in the triangular cylinder GDFG'D'F' from the wall form the row matrix

$$g_{w_+} = S \cdot (0, -\frac{1}{R_{el}} \cdot \frac{\partial u}{\partial y}, p - \frac{4}{3R_{el}} \cdot \frac{\partial v}{\partial y}, 0)_{Q_+} \quad (9)$$

On the other hand, the same four fluxes entering into the fluid in the triangular cylinder EFDE'F'D' from the wall form the row matrix

$$g_{w_-} = -S \cdot (0, -\frac{1}{R_{el}} \cdot \frac{\partial u}{\partial y}, p - \frac{4}{3R_{el}} \cdot \frac{\partial v}{\partial y}, 0)_{Q_-} \quad (10)$$

Using the mirror image conditions, we have

$$(\frac{\partial u}{\partial y})_{Q_-} = -(\frac{\partial u}{\partial y})_{Q_+}, \quad (p - \frac{4}{3R_{el}} \frac{\partial v}{\partial y})_{Q_-} = (p - \frac{4}{3R_{el}} \frac{\partial v}{\partial y})_{Q_+} \quad (11)$$

By using Eqs. (9-11), it is concluded that the mass, momentum, and energy fluxes entering into the fluid in GDEFG'D'E'F', i.e., $CE^{(1)}$, from the wall form the row matrix

$$g_w = g_{w_+} + g_{w_-} = -2S \cdot (0, \frac{1}{R_{el}} \cdot \frac{\partial u}{\partial y}, 0, 0)_{Q_+} \quad (12)$$

In the current treatment, the surviving x-momentum flux in Eq. (12) is treated as a source term in flux balance calculation involving conservation element $CE^{(1)}$. To calculate the flux g_w , we need to calculate $\partial u / \partial y$. For simple laminar flows with enough mesh resolution of the boundary layer, because $u = 0$ at point Q_+ , and $u \equiv (u_G + u_{G'})/2$ at the midpoint M of $\overline{GG'}$, we assume

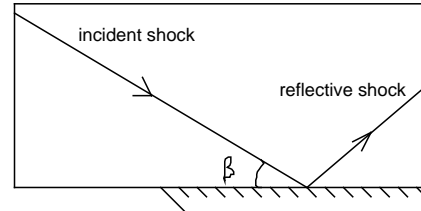


Fig.3 Shock/boundary layer interaction problem.

$$\left(\frac{\partial u}{\partial y} \right)_{Q_+} \approx \frac{(u_G + u_{G'})/2 - 0}{y_M - y_{Q_+}} \quad (13)$$

Note that, $g_w = 0$ for inviscid flows, and the current treatment becomes the usual "slip" condition. As such, the present boundary treatment is suitable for inviscid as well as viscous flows. Although not shown, the above solid boundary condition has been extended to sloping and curved surfaces.

4 Numerical Results

Figure 3 is a schematic of a standard test problem for Navier Stokes solvers. When the shock is strong and the incident shock angle is large enough, boundary layer separation occurs at the shock impinging point. It is assumed that $M_\infty=2.0$, $R_e=2.96\times 10^5$ and $\beta=32.6^\circ$. The computational domain is $[0, 0.12] \times [0, 0.06]$. Clustered cells near the solid wall are employed to resolve the boundary layer. Here 28800 isosceles triangles are used.

The new solid boundary treatment is applied along the wall. In the left and upper boundaries, the flow conditions are fixed according to the incoming flows. Non-reflective boundary condition is used in the outlet boundary. The numerical results are shown in Fig. 4 for pressure contours, pressure distribution and skin friction distribution along the wall. The negative skin friction coefficient represents the recirculating flow region. The numerical results, including the separation location and length, compare favorably with the experimental data [4,5].

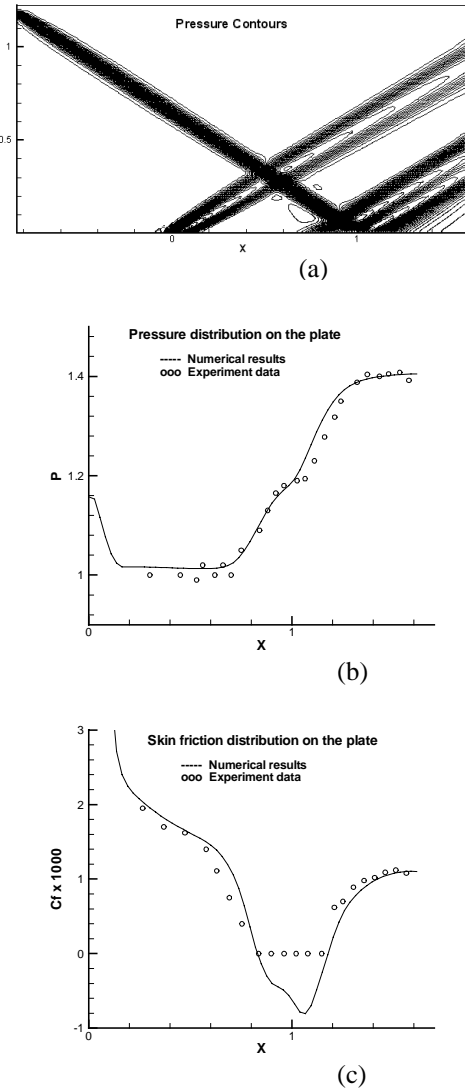


Fig.4 Numerical and experimental results of the shock/boundary layer interaction: (a) pressure contours, (b) pressure distribution along the wall, and (c) skin friction distribution along the wall.

The second example is an inviscid shock reflection problem [6]. This problem has exact Euler solution. We apply the same wall boundary condition treatment with $I/R_{eL} \rightarrow 0$. A uniform mesh of 9600 conservation elements is used. The numerical results are shown in Fig.5. These results agree very well with the analytical solutions.

5 Concluding Remarks

A unified wall boundary treatment for viscous and inviscid flows has been described. In this treatment, the wall boundary condition for inviscid flows becomes a special case of that for viscous flows. Numerical results show that this new boundary treatment is robust, efficient, and very accurate for viscous as well as inviscid flows. This new treatment could also be easily extended to model complex flow physics along walls, e.g., flow permeation through a porous wall.

References

1. S.C. Chang: "The Method of Space-Time Conservation Element and Solution Element – A New Approach for Solving the Navier Stokes and Euler Equations," *J. Comp. Phys.*, **119**, pp. 295-324 (1995)
2. S.C. Chang, X.Y. Wang and C.Y. Chow: "The Space-Time Conservation Element and Solution Element Method: A New High-Resolution and Genuinely Multidimensional Paradigm for Solving Conservation Laws," *J. Comp. Phys.*, **156**, pp.89-136 (1999)
3. S.C. Chang, S.T. Yu, A. Himansu, X.Y. Wang, C.Y. Chow and C.Y. Loh: "The Method of Space-Time Conservation Element and Solution Element – A New Paradigm for Numerical Solution of Conservation Laws," *Computational Fluid Dynamics Review 1998*, edited by M.M. Hafez and K. Oshima (World Scientific, Singapore 1998), vol. 1, pp. 206-240.
4. R.J. Hakkinen, I. Greber, L. Trilling and S.S. Abarbanel: "The Interaction of an Oblique Shock Wave with a Laminar Boundary Layer," NASA Memo 2-18-59W (1959).
5. Yee, H.C., Warming, R.F. and Harten, A., "Implicit Total Variation Diminishing (TVD) Schemes for Steady-State Calculations," AIAA paper 83-1902 (1983)

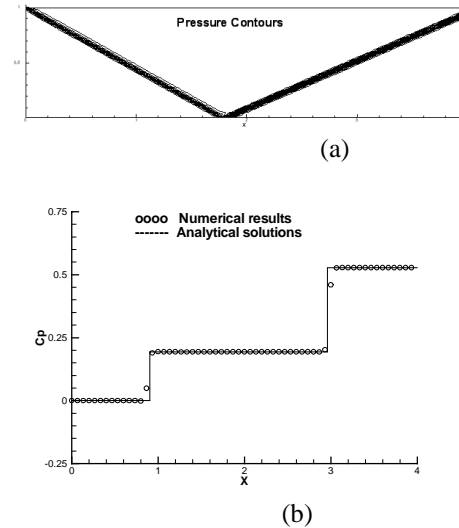


Fig.5 Euler solutions of the oblique shock reflection problem. (a) Pressure contours; (b) Pressure coefficients at the mid-section of the computation domain